MAPPING WATER ICE CLOUDS (AND OZONE) WITH MRO/MARCI.

M. J. Wolff, *Space Science Institute, Boulder, CO, USA (mjwolff@spacescience.org)*, **R. T. Clancy,** *Space Science Institute, Boulder, CO, USA*, **B. Cantor**, *Malin Space Science Systems,* **J-B. Madeleine**, *Laboratoire de Météorologie Dynamique, CNRS/UPMC/IPSL, Paris, France*.

Introduction: The profound effects of dust aerosols on the structure and behavior of the Martian atmosphere were recognized early in the spacecraft era [1]. Not surprisingly, a large fraction of atmospheric observational studies have focused on characterizing the distribution and properties of the dust aerosol particles [2, and references therein]. However, several less well studied components of the Martian atmosphere are now recognized as playing an important role in atmospheric dynamics and evolution, either directly as in the case of water ice clouds [3,4] or more passively as a sensitive tracer as in the case of ozone [5,6]. Despite the (relatively) recent elevation of interest in water ice clouds and ozone abundances (and subsequent studies enabled by spacecraft observations [e.g., 2]), what has been lacking is a dataset with systematic observations that are global in spatial extent and span multiple Martian years. Fortunately, such a dataset now exists.

The Mars Color Imager (MARCI) instrument onboard the Mars Reconnaissance Orbiter (MRO) obtains near-global coverage of Mars on a daily basis [7]. This degree of spatial and temporal sampling offers one the ability to characterize seasonal and inter-annual variations atmospheric processes. Of specific interest for studies of water ice clouds and ozone abundances is the presence of the two ultraviolet (UV) bands. These two channels were chosen to exploit the reduced surface contrast and increased atmospheric contribution (via scattered radiance), as well as for the sensitivity (in one band) to the Hartley ozone band. Consequently, MARCI observations can provide global maps of water ice optical depth and ozone column abundances on a daily basis.

In our presentation, we outline the MARCI dataset and retrieval algorithms employed for the generation of the water ice and ozone column maps. In addition, we highlight some initial results that focus on the seasonal behavior of water ice clouds; ozone results will be presented elsewhere [8]. Finally, we will provide spot comparisons for our results with those of recent spacecraft observations including MEX/SPICAM [9] and MEX/OMEGA [10].

The MARCI Dataset: The MARCI instrument is a wide-angle, 7-color ``push-frame'' imager whose overall components, capabilities, and performance (including calibration methodology) are described in great detail by [7,11] with updates for the UV provided by [12]. For our purposes here, it will suffice to recount a few important details.

The solar irradiance-weighted centroids of the two UV channels are 263 nm and 321 nm for the so-called "Band 6" and "Band 7," respectively. The associated photometric accuracies are ~10% (Band 6) and ~8% (Band 7), with the photometric precision being 2-3%.

MARCI acquires 12 or 13 mapping strips per day at a local time (on the equator) of ~15h. The intrinsic resolution of a UV image is ~8 km per pixel at nadir. While this provides "global coverage" in the sense that entire planet is uniformly sampled in latitude, the altitude of the orbit prevents one from producing seam-free retrieval maps.

Modeling Algorithms and Methodology: The retrieval of water ice optical depth and ozone abundance is accomplished using a rigorous multiple-scattering radiative transfer formalism. To a large extent, the individual components and prescriptions for the relevant atmospheric state variables has been previously developed by [12]. Here, we present only a brief summary of the various algorithms and input value specifications.

Radiative Transfer. The core of our radiative transfer calculations is once again based upon the DISORT public domain package [13]. The primary difference with that of [12] is that we avoid the computational overhead of on-the-fly solutions of the radiative transfer problem. Instead, we construct a large lookup table (LUT) of radiative transfer models. Each of the input parameters is tessellated sufficiently to avoid introducing granularity-based errors. The result is individual LUTs that are approximately 550 MB and 200 MB for Bands 6 and 7, respectively.

Surface Reflectance. For the non-ice surface, we employ the "Hapke-function" model developed for the UV dust analyses of [12]. At present, we also assume that the Hapke *w* parameter is spatially uniform, though the retrieval results indicate that a spatially-variable approach should produce better results. For the ice-covered surfaces, we employ a simple Lambert model of the type used for Hubble Space Telescope UV analyses [e.g., 14]. However, the actual albedo values are determined as part of the retrieval process. Due to the inability of MARCI data to usefully discriminate between surface and atmospheric ice, we cannot produce accurate ice optical depths over ice surfaces.

Aerosol Model. For dust, we simply adopt the non-spherical model results of [12] under the as-

sumption that r_{eff}=1.5 μm is representative of all conditions sampled. The vertical profile is assumed to that of uniform mixing.

For water ice particles, the situation is more complicated. Typical terrestrial crystal habits – hexagonal prisms and associated shapes -- do not seem to provide a good representation of Martian water ice aerosols, e.g. [15]. However, recent work reveals that even on the Earth, ice particles of the size found on Mars (1-5 μm) are likely to be polycrystalline [16]. Such a "shape" led [17] to propose that such particles might be adequately represented by a droxtal, which is a generalization of a hexagonal prism. See Figure 1. The extra facets can provide a significantly different angular scattering pattern.

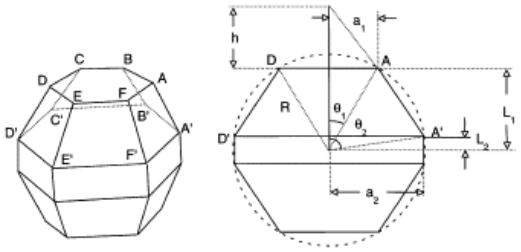

Figure 1 -- Droxtal shape, proposed for small ice crystals by [17], adopted from their Figure 4.

To calculate the scattering properties of a droxtal, we use the discrete dipole approximation (DDA) public domain code, DDSCAT [18]. We perturb the shape parameters from those of [17] by requiring that any structure in the retrieval maps does not correlate with phase angle. That is to say, a mismatch between the model and actual phase function of sufficient amplitude will introduce artifacts that follow contours in phase angle (and we did so unintentionally repeatedly during our iteration on the droxtal parameters). Our current retrieval algorithm adopts an r_{eff}=3 μm and assumes that water ice is uniformly mixed above the water vapor saturation altitude.

Ozone Vertical Profile. The absolute values of the ozone column densities are typically sensitive to the vertical mixing profile employed. In the absence of any observational constraint on this parameter, we resort to the ozone vertical mixing profiles predicted by the LMD global circulation model photochemistry package [6]. At present, we allow for seasonal variability through a series of 12 profiles equally spaced throughout the Martian year.

Atmospheric State. As with [12], we adopt the atmospheric state variables of temperature, surface pressure, and dust optical depth from a TES-based climatology. The connection of pressure with altitude surfaces is accomplished through an integration of the hydrostatic equation. Surface elevation (i.e. surface pressure) variability across each strip is treated through a simple scaling of the equation of state using a MOLA topography and an atmospheric scale height of 10 km.

The next version of the retrieval algorithm is anticipated to implement an MRO-based climatology/database: dust optical depth from CRISM and temperature from MCS.

Individual Parameter Retrieval. In contrast to the approach of a non-linear minimization used in [12], we employ the operation of N-dimensional linear interpolation. By prescribing the photometric and atmospheric state variables, one can construct a hypercube, reduced in size from the initial LUT through the use of the bracketing points for each input parameter. The resulting hypersurface then provides a one-to-one mapping of I/F to the desired retrieval parameter. However, it is important to note that *this process requires that the relation between I/F and the parameter be monotonic*. Fortunately, for the MARCI viewing geometry, increasing the optical depth of water ice or column abundance of ozone produces a unidirectional change for the range of parameter values considered "retrievable" (optical depth < 4, ozone columns < 60 μm-atm). This is in contrast to dust aerosols where a distinct lack of monotonicity can be observed for surface reflectance values in the regime of low-to-moderate dust optical depths.

Retrieval Mapping Procedure. For each day of MARCI observations, the retrieval products are constructed as follows:

1. An on-the-fly calibration of the MARCI data from Data Number to I/F is performed for each Band 6 and 7 strip, typically 12 or 13 for each band.
2. The "backplanes," or metadata, are generated for each pixel in the I/F images: photometric angles, elevation, surface pressure map, dust optical depth.
3. The water ice optical depth retrieval is performed using the Band 7 data.
4. An ozone column abundance retrieval is done for each Band 6 strip using the ice optical depths of Step 3 and the Hapke surface assumption.
5. A Lambert surface albedo retrieval is done with the Band 7 images under the assumption of no aerosol loading.
6. A second ozone column abundance retrieval is performed on the Band 6 data, now assuming no aerosols and a Lambert surface with the pixel albedo values derived in Step 5.
7. A polar mask is calculated from the results of Step 5 and imposing latitude and I/F cutoffs values.
8. A final ozone product is constructed using the polar mask to combine the results of Steps 4 and 6.

It takes approximately 1.75 hours of processing time for a single mapping day using a single core of 3.0 GHz "Nehalem" chip (on a 2008 era Xserve). An example of this process for the water ice cloud retrieval is shown in Figure 2 (ozone examples will be shown by [8]). Consequently, keeping up with new observations is not a problem, but reprocessing the dataset from the beginning of the mapping phase (early November 2006) does require the use of multiple processors.

In addition to updating the climatology scheme, as mentioned above, several improvements in the current algorithm are planned: spatial variability of the Hapke *w* parameter, (coarse) spatial variability in the ozone profile, weighted temporal and spatial averages in the ozone column abundances to avoid discrete edges in the retrieval maps (i.e., moving one pixel or strip can introduce the switch to a different lookup table or vertical profile assumption). These modifications should appreciably improve the resulting retrieval products, though it is likely that they will (at least) double the above processing time. Thus, parallel processing will likely need to be implemented for the general retrieval algorithm.

Uncertainties: For the current version of the retrieval, we estimate the uncertainty in the ice optical depth to be in the range 0.02-0.03 with the detection threshold of about 0.05. For ozone, the precision is about 1-2 μm-atm with the detection threshold being approximately the same magnitude.

Results: The above process produces a large amount of primary (water ice optical depth, ozone column depths) and secondary (input values, quality flags, masks, etc) data products. Even when stored as integers and compressed, the data volume for a typical day (13 orbits) is about 100 MB. Clearly, these products need to be managed, and perhaps further condensed, for use by an interested user (including us)!

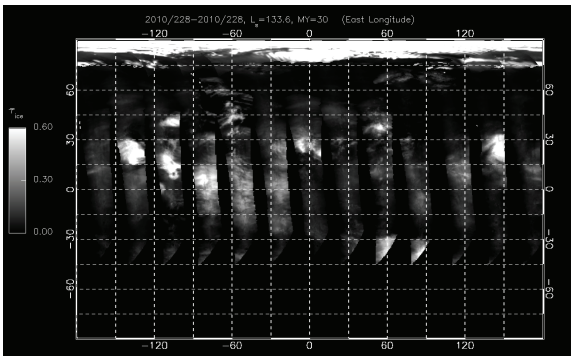

Figure 2 – Sample cloud map for day 2010-233, mid-summer in the Northern Hemisphere. The bright region in the north polar region is the result of assuming a dark surface, i.e., the retrieval produces thick clouds wherever there is surface ice. Before ingestion into a database product, one would apply a polar mask to remove such pixels from consideration. The cylindrical projection is a display convention; the retrieval products retain the geometry of the original MARCI image.

We are currently exploring several formats for the distribution of these products to users. Along these lines, we are actively developing a Twiki site (https://gemelli.spacescience.org/twiki/bin/view/MarsObservations/MarciObservations/) that allows for product download (at the moment, only graphical summaries of the daily retrievals, for both clouds and ozone; similar to the format of Figure 2). An additional goal of this site is to solicit community participation in both feedback in terms of desired data products/format, as well as to increase the content of the site itself (registered users can be added to a list that allows editing of this site and associated topics).

For the next step in providing retrieval products, we are currently working with a pixel-binning scheme using 64 km sized bins (roughly 1 pixel per degree). In this format, one can condense the basic retrieval information for the current mapping dataset to approximately 1 GB (allowing for storage as scaled integers and gzip compression).

Clearly, data dissemination mechanisms and issues of format are areas of active work by the authors. As such, we welcome feedback, including requests for various data formats, summary products for limited periods of time (perhaps the only tractable way to tabulate the 8km pixel mode data).

Applications: There are many possible applications for the MARCI mapping data products. Several will be discussed during our presentation or by other presentations, including:

1. Time series studies of cloud optical depths at specific regions of interest. An example of this is being presented regions near and around the north polar region during the summer season; see presentation by Haberle et al. [19].
2. Seasonal ozone behavior in the polar regions, as well as more global annual behavior in connection with other MRO datasets; see presentation by Clancy et al. [8]
3. Characterizing annual behavior in the water ice cloud cycle. For the purposes of climatology, and perhaps comparisons to Global Circulation Models, one can utilize zonally averaged retrievals. An example of this can be seen in Figure 3, where the evolution of the aphelion cloud belt for the period of mid-spring through mid-summer (in the northern hemisphere) is compared for Mars Years 29 and 30. Note the weaker cloud belt in Mars Year 29, which is the spring immediately

following the planet encircling dust event of Year 28.

4. A comparison of MARCI retrievals with those reported for SPICAM [9] and OMEGA [10].

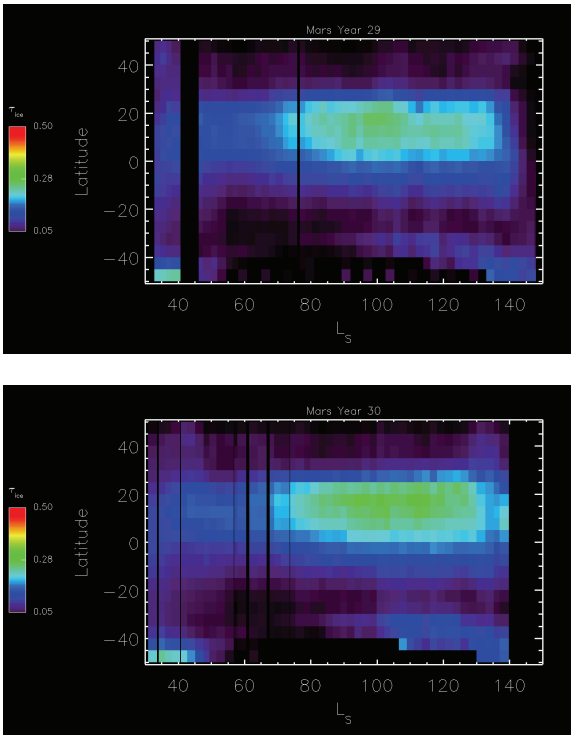

Figure 3 -- Behavior of aphelion cloud belt in Mars Years 29 (top) and 30 (bottom). Note that although physical location of the cloud belt remains essentially unchanged, the strength of the feature is weaker in Mars Year 29.

Acknowledgements: This work was supported by NASA through the MRO Project and a contract to Malin Space Science Systems (JPL Contract 1275776). Travel support for MJW provided by MDAP grant NNX10AO23G.

References: [1] Gierasch, P. J., and R. M. Goody, Planet. Space Sci., 16, 615– 646, 1968. [2] Smith, M. D., Annu. Rev. Earth Planet. Sci., 36, 191 – 219 2008. [3] Clancy, R. T. et al., Icarus 122: 36-62, 1996. [4] Montmessin, F. et al., JGR (Planets), 109, 0004, 2004. [5] Clancy, R. T. and H. Nair, JGR, 101, 12785-12790, 1996. [6] Lefèvre et al., Nature, 454, 305-309, 2008. [7] Malin, M., et al., Icarus, 194, 501-512, 2008. [8] Clancy, R.T. et al, this meeting. [9] Mateshvili, N. et al., Planetary and Space Science 57: 1022-1031, 2009. [10] Madeleine, J-B. et al., submitted. [11] Bell, J. et al, JGR Planets, 114, E08S92, 2010. [12] Wolff, M. et al., Icarus, 208, 143-155, 2010. [13] Stamnes, K. et al., Appl. Opt. 27, 2502–2509, 1988. [14] Clancy, R. T. et al, Icarus 138: 49-63, 1999. [15] Clancy, R. T. et al, JGR (Planets), 108, 5098, 2003. [16] Bailey, M. and B. Hallett, J. Atm Sci, 66, 2888, 2009. [17] Yang, P. et al., 79, 1159, 2003. [18] Draine, B. T. and P. Flatau, http://arXiv.org/abs/1002.1505v1, 2010. [19] Haberle, R. M. et al., this meeting.